NANOSYSTEMS: PHYSICS, CHEMISTRY, MATHEMATICS, 2014, 5 (4), P. 477–485

CHLORGRAPHYNES: FORMATION PATH, STRUCTURE AND ELECTRONIC PROPERTIES

A. L. Ivanovskii, A. N. Enyashin

Institute of Solid State Chemistry UB RAS, Ekaterinburg, Russia

enyashin@ihim.uran.ru

PACS 61.48.Gh, 68.43.-h, 73.22.Pr, 81.05.ue

The presence in graphyne sheets of a variable amount of sp^2 and sp^1 carbon atoms suggests a high ability of these nanostructures for saturation. E.g., covalent binding of chlorine atoms would lead to sp^3- and new sp^2 hybridized carbon atoms, and the emergence of chlorgraphynes (chlorinated graphynes) with variable Cl/C stoichiometry may be expected. Here, employing DFT band structure calculations, a series of new graphyne derivatives — layered chlorgraphynes — is examined on example of α-graphyne. The possible formation path of chlorgraphynes as a set of consecutive free-radical additions of Cl atoms is established. From examples of a few representative compounds, the trends in the structural and electronic properties are discussed, depending on their stoichiometry.

Keywords: Graphynes, carbon allotropes, graphene derivatives, DFT calculations.

Received: 16 June 2014
Revised: 30 June 2014

1. Introduction

Graphene, a two-dimensional (2D) mono-atomic-thick sheet of sp^2 hybridized carbon, exhibits a unique combination of structural, mechanical, electronic and thermal properties [1,2]. It is viewed today as an advanced material for use in a vast range of nanotechnology applications [3-5]. However, "graphene is not the end of the road"; and numerous efforts have been focused recently on the search for graphene-based materials with novel functionalities [6], particularly, through adsorption of various atoms or molecules onto the surface of graphene [7,8]. For example such atoms as fluorine, oxygen, or hydrogen adsorbed on graphene can form covalent bonds with the carbon atoms, which lead to a change in the hybridization state of C atoms from sp^2 to sp^3 and may provoke the opening of a band gap. In this manner, fluorination of graphene gives rise to the wide-band-gap 2D crystals, which were termed *fluorographenes* [9]. A set of outstanding chemical and physical properties for single-layered fluorographenes has been already found experimentally and predicted theoretically [8-17]. These materials, with a variable F/C content (up to the stoichiometry CF), may be considered as a promising platform for further applications.

At the same time, the versatile flexibility of carbon to form a few competing hybridization states allows one to design numerous types of flat single-atom-thick carbon networks: so-called graphene allotropes [18]. One of interesting families of these allotropes is represented by so-called *graphynes*, which can be described as graphene lattices, where some or all aromatic =C=C= bonds are modified by the insertion of acetylenic linkages (–C≡C–) [19]. These carbon (sp^2+sp^1) sheets with a high level of π-conjunction, with uniformly distributed pores, and with density much less than that of graphene, possess unusual electronic properties, nonlinear optical susceptibility, thermal resistance, conductivity, and through-sheet transport of ions [20-23]. Currently, they are considered as promising materials for nanoelectronics, for hydrogen storage, as membranes (for example, for hydrogen separation from syngas — as an alternative of the graphene nanomesh), for energy storage applications or as candidates for the anode materials in batteries [24-26]. Tuning of these materials' properties should be critical for their further application. Analogously to graphene, it might be achieved using surface chemisorption of hydrogen or fluorine atoms [13,14,16,17]. Quantum-chemical calculations demonstrate that the electronic and transport properties of modified carbon layers should be very sensitive to the surface arrangement of adsorbed atoms. Yet, both experimental and theoretical work show that the formation of a desired configuration of ad-atoms on the layers cannot be released in the large scales and has mainly casual character.

While the hydrogen, fluorine and oxygen derivatives of graphene and graphyne layers are profoundly studied, the information about other possible types of derivatives is lacking. In contrast to H or F atoms, Cl atoms have larger atomic radii. The latter magnifies the role of steric factors and may lead to a more selective chemisorption of ad-atoms, i.e. to a narrower family of possible types of modified layers. Herein, we theoretically explore the structural, electronic properties and stability for the consequence of hypothetical chlorinated graphynes (*chlorgraphynes*), which could be fabricated by chlorination of a graphyne layer and could become likely candidates for the engineering of novel electronics materials.

2. Computational details

All calculations were performed by means of the density functional theory (DFT) [27] using the SIESTA 2.0 code [28,29] within the local-density approximation (LDA) with the exchange–correlation potential in the Perdew-Zunger form [30]. The core electrons were treated within the frozen core approximation using norm-conserving Troullier–Martins pseudopotentials [31]. The valence electrons were taken to be $2s^22p^2$ for C and $3s^23p^5$ for Cl. The pseudopotential core radii were chosen as suggested by Martins and equal to 1.50 and 1.54 bohr for s- and p-states of C, and 1.75 bohr for both $s-$ and p-states of Cl. In all calculations, only single-ζ basis set was used for all atoms. For k-point sampling, a cutoff of 10 Å was used [32]. The k-point mesh was generated by the method of Monkhorst and Pack [33]. A cutoff of 350 Ry for the real-space grid integration was utilized. All calculations were performed using variable-cell and atomic position relaxation, with convergence criteria set to correspond to the maximum residual stress of 0.1 GPa for each component of the stress tensor, and the maximum residual force component of 0.01 eV/Å. Initial interlayer spacing along c-direction of a hexagonal or an oblique lattice was set to 50 Å.

As a representative of graphyne layers, the layer of α-graphyne (so-called *supergraphene*) was selected (Fig. 1). This hexagonal carbon network consists of sp^2-hybridized C atoms interlinked via dimers of sp-hybridized C atoms and contains 8 atoms per unit cell. A possible reaction path for the full chlorination of α-graphyne was established as a set of consecutive free-radical additions of single Cl atoms. At every step of the reaction path all possible variants of Cl atom anchoring to the carbon atoms were analyzed. Afterwards, the most stable isomer found served as the ancestor for the next step. In total, the chlorgraphynes with stoichiometric compositions C_8Cl_n (n = 1 – 14) and different ordering of Cl atoms were taken into consideration, which required calculations for 78 compounds.

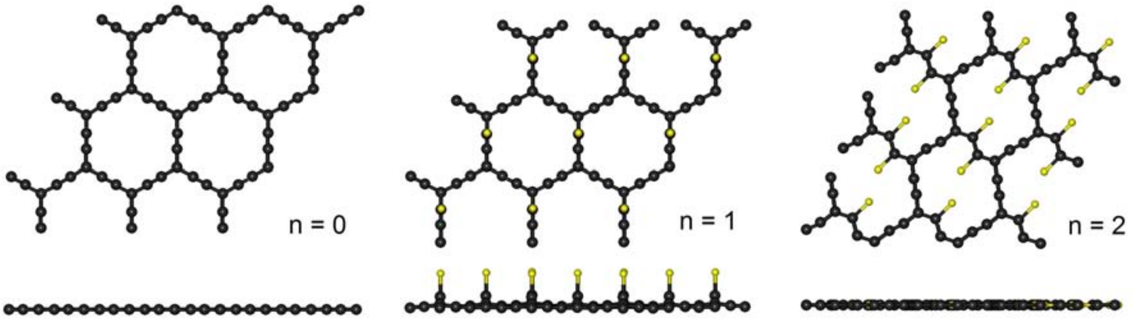

Fig. 1. Optimized atomic structures for the layers of pure α-graphyne (n=0) and the most stable isomers of chlorgraphynes C_8Cl_n with low Cl content (top and side views are depicted)

3. Results and Discussion

3.1. Electronic structure of pure α-Graphyne

The first clue about the reactivity of α-graphyne can be found from the analysis of the band structure. In terms of electronic structure, lattice symmetry and chemical bonding, pure α-graphyne is the closest relative of graphene. Hexagonal network of α-graphyne possesses the picture of band structure with characteristic crossing of the bands at the Fermi level in K-point (Dirac cones) (Fig. 2). The near-Fermi bands are composed of states from the broadly conjugated π-system of $2p_z$C-orbitals from both sp^2- and sp-hybridized C atoms. Both features should provide semimetallic type of conductivity and superior mobility of electrons in α-graphyne similar to those in the graphene [18].

However, in contrast to the graphene, the band structure of α-graphyne is characterized by bands with clearly low dispersion at 2.5 eV below the Fermi level. These bands are associated exclusively with $2p_y$C-orbitals from the dimers of sp-hybridized C atoms and are responsible for the formation of second π-bond network within the carbyne groups. $2p_y$C-orbitals are united in couples and are fairly localized in the plane of layer, barely overlapping with orthogonal $2p_z$C-orbitals.

The presence of two types of π-bonding suggests the different reactivity of sp^2- and sp-hybridized C atoms in α-graphyne. The formation of chemical bonding between an adatom and carbon layer by means of a $2p_z$C-orbital should imply an essential interference into the aromatic-like π-system due to the appearance of sp^3-hybridized C atom and cannot be favorable in framework of this classical concept. In turn, the chemical bonding to the orthogonal π-bond consisting of $2p_y$C-orbitals between two sp-hybridized C atoms does not perturb the conjugation of this π-system and is accompanied only by the rupture of one π-bond. The preliminary comparison of the total energies for α-graphyne with single Cl atom bounded covalently either to sp^2- or to sp-hybridized C atoms (C_8Cl chlorgraphyne) confirms this conjecture: the second type of chemisorbate is more stable on 0.545 eV per Cl-atom.

3.2. Electronic structure and stability of lower Chlorgraphynes (C_8Cl and C_8Cl_2)

In order to elucidate the stability of different chlorgraphynes in more detail, the theoretical energies of formation ΔE_n were estimated assuming formal reactions: C_8(graphyne)

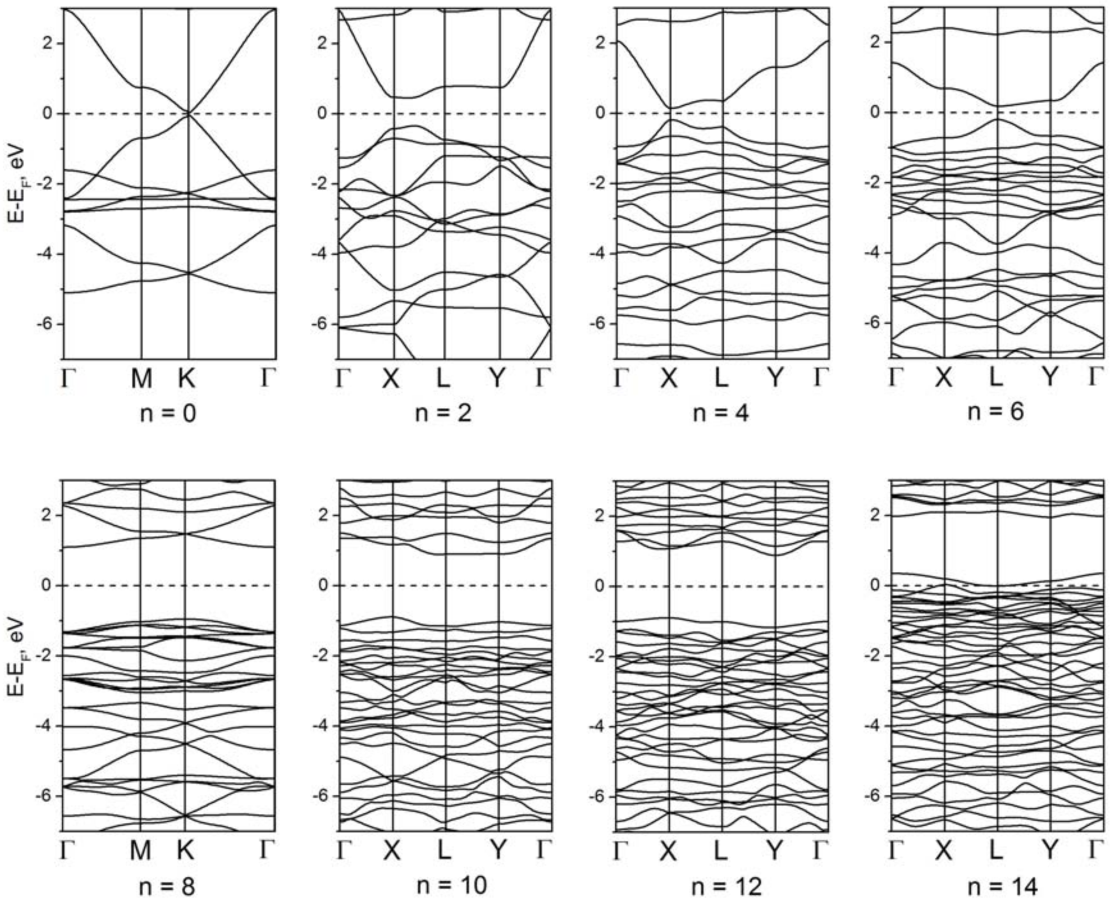

n = 0 n = 2 n = 4 n = 6

n = 8 n = 10 n = 12 n = 14

FIG. 2. Band structures of pure α-graphyne (n = 0) and the most stable isomers of chlorgraphynes C_8Cl_n

+ $(n/2)Cl_2 = C_8Cl_n$, and the values of E_{form} were calculated as: $\Delta E_n(C_8Cl_n) = [E_{tot}(C_8Cl_n) - (n/2)E_{tot}(Cl_2) - E_{tot}(C_8(\text{graphyne}))]/n$, where E_{tot} are the total energies of the corresponding substances as obtained in our calculations. Within this definition, a negative value of ΔE_n indicates that it is energetically favorable for given reagents to form stable phases, and *vice versa.* The calculations of ΔE_n performed for more than 70 structures of different composition depending on their constitutional and conformational isomerism reveal a quite strong influence of both electronic and steric factors on the stability of chlorgraphynes' series.

All the stablest chlographynes of different stoichiometry are characterized by the negative values of the formation energy ΔE_n, i.e. the saturation of graphyne network with the formation of covalent C–Cl bonds is an exothermic process favored by electronic factors (Fig. 3). E.g., the value ΔE_n for the stablest isomer of aforementioned C_8Cl chlorgraphyne with anchoring of Cl atom to *sp*-hybridized C atom is about –0.35 eV/Cl-atom, while anchoring to sp^2-hybridized C atom is endothermic and requires at least +0.20 eV/Cl-atom.

The chemisorption of additional Cl atoms with the formation of C_8Cl_2 chlorgraphyne may be highly favorable, when it is released in the structure shown in Fig. 1 (n = 2). This isomer of C_8Cl_2 chlorgraphyne possesses a unique structural motif. Like graphene or α-graphyne layers it is a single-atom thick layer. All Cl atoms of this structure are lodged in the trans-position at ethylidene bridges and within the plane of C atoms. In this manner, the structure preserves as much as possible the system of conjugated π-bonds formed by

$2p_z$C-orbitals, as in the parent graphyne and consists of planar 18-membered rings, yet, in an oblique conformation. Despite the hexagonal nature of α-graphyne, the electronic structure of C_8Cl_2 chlorgraphyne is characterized by a band gap opening of about 0.78 eV and a greater dispersion of the bands (Fig. 2, n = 2). Meanwhile, the new peak of $3p$Cl states arises at 3.5 eV below the Fermi level, while the top of valence band and the bottom of conduction band are still composed of $2p$C states (Fig. 4).

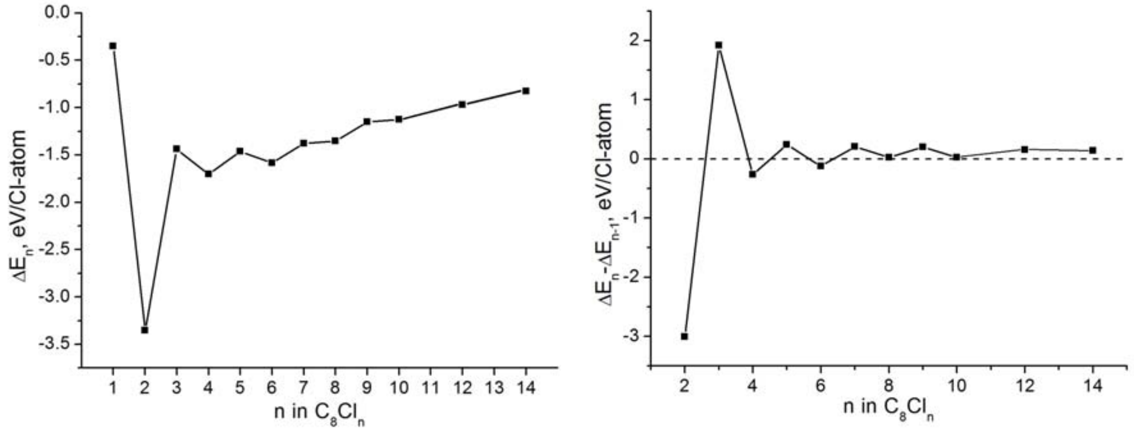

FIG. 3. Formation energies ΔE_n for the most stable isomers of chlorgraphynes C_8Cl_n and their relative difference depending on the stoichiometry

3.3. Electronic structure and stability of higher Chlorgraphynes ($C_8Cl_{3\text{-}14}$)

In fact, further saturation of graphyne network follows the same trends as for the formation of lower chlorgraphynes. Any next addition of Cl atoms with the formation of covalent C-Cl bond proceeds with the least possible violation of the conjugation between $2p_z$C-orbitals (Fig. 5). In the first steps, the consecutive anchoring of Cl atoms to the sp-hybridized C atoms should be obtained by means of bonding with $2p_y$C-orbitals in trans-position, which releases chlorgraphynes with the compositions up to C_8Cl_6. It is noteworthy that at this stage, the chlorination process is already considerably affected by steric factors. A major part of added Cl atoms cannot be placed into the hole of the 18-membered ring. Rotational displacement of planar bridging groups of C=C bonds can be observed, when the Cl atoms come out of the plane of graphyne. Yet, the π-conjugation of $2p_z$C-orbitals still remains. Even-numbered chlorgraphynes are semiconductors with relatively narrow band gaps (0.34 eV for C_8Cl_4 and 0.37 eV for C_8Cl_6, Fig. 2). The near Fermi states are represented by $2p_z$C states like in the parent phases. The relative intensity of the $3p$Cl states on the DOS profile increases in strength (Fig. 4, n = 4 and 6). They demonstrate splitting and have higher energies, than those in planar C_8Cl_2, which is evidence for a weaker overlap between the $3p$Cl states and the conjugated system of π-bonds.

Subsequently, calculations have proven that the anchoring of Cl atoms would likely proceed by means of $2p_z$C-orbitals of initially sp^2-hybridized C atoms with emergence of sp^3-hybridized C atoms, which breaks π-conjugation in the network of double C=C bonds (formerly, carbyne dimers) (Fig. 5, n = 8). Obviously, this process is driven mainly by steric factors and Cl atoms settle on the C atoms with a larger available space. A comparison of relative formation energies between the conformers of the C_8Cl_7 and C_8Cl_8 chlorgraphynes corroborates, that the steric effects should play also a major role in the conformer stability of these molecular networks. The most stable conformers should possess minimal strain energy of the layers due to symmetric structure and the ratio of Cl atoms chemisorbed from different sides as close as to 1:1. The occurrence of new type of sp^3-hybridized C atoms in the chlorgraphyne layer and complete destruction of the π-conjugation are accompanied by the emerging of new band of $3p$Cl states near the top of valence band and a considerable increase of the band gap to 2.2 eV (Fig. 4, n = 6).

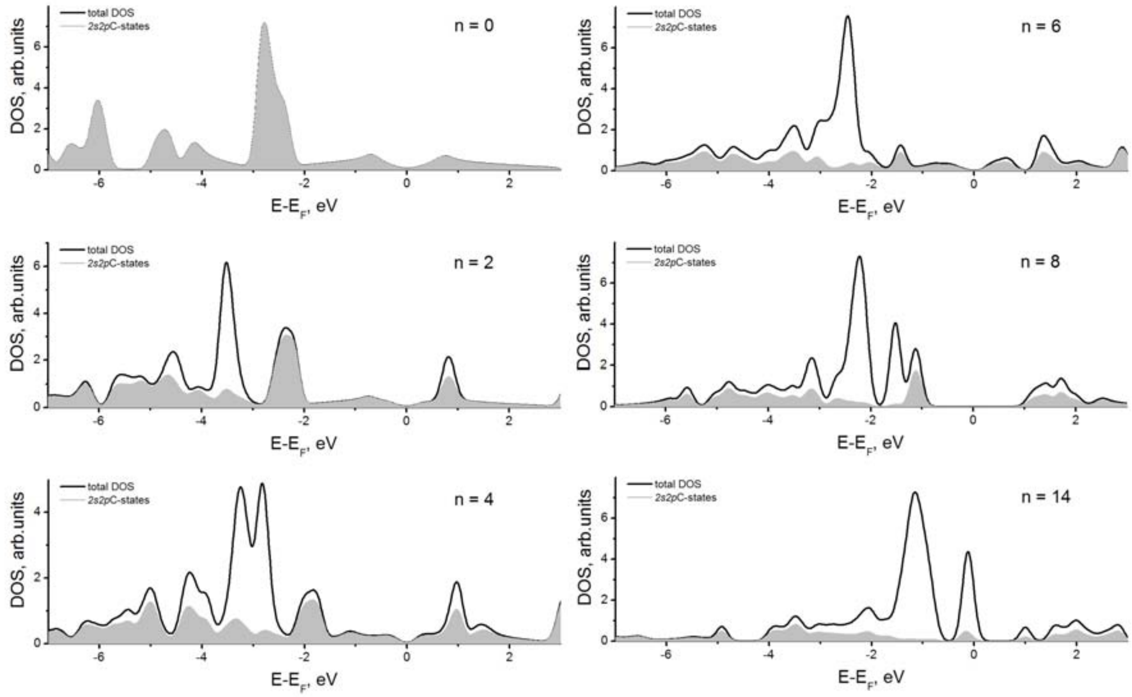

FIG. 4. Total and partial spC densities of states for a few of the most stable isomers of chlorgraphynes C_8Cl_n depending on the Cl content

The formation of higher chlorgraphynes C_8Cl_n with n up to 14 is possible only by the anchoring of Cl atoms to the rest of C=C bonds of former carbyne bridges (Fig. 5). The arrangement of Cl atoms within these structures can be characterized as strongly staggered at all carbon atoms fragments and as always *anti*-conformic at forming $-CCl_2-CCl_2-$ bridges, which provides the minimal energy of the steric stress. Despite the negative formation energy values, these chlorgraphynes demonstrate an essential stretch of the carbon network with an essential increases in the C–C bond lengths, which cannot be attributed to kinetically stable systems. The C–C bond lengths increase gradually from α-graphyne to C_8C_8 chlorgraphyne, but do not exceed the values for classical C–C bonds of different order in hydrocarbon compounds. For example, the bond lengths between atoms of different hybridization in α-graphyne are equal to 1.44 and 1.27 Å for sp^2C–spC and spC–spC bonds, respectively. After chlorination and change of hybridization, these bond lengths become 1.46 and 1.45 Å in C_8Cl_2, 1.50 and 1.42 Å in C_8Cl_6 and 1.56 and 1.40 Å in C_8Cl_8, respectively. In the fully chlorinated α-graphyne, C_8Cl_{14} chlorgraphyne, these bond lengths are 1.72 and 1.66 Å, which is much greater than the 1.55 Å for sp^3C– sp^3C in alkanes. Indeed, the geometry optimization of C_8Cl_{14} chlorgraphyne never was finished with a pure covalently bounded structure and a part of Cl atoms always can be found as physisorbed at the C_8Cl_{12} layer (Fig. 5, n = 14). The latter can be proven by the picture of DOS distribution: the Fermi

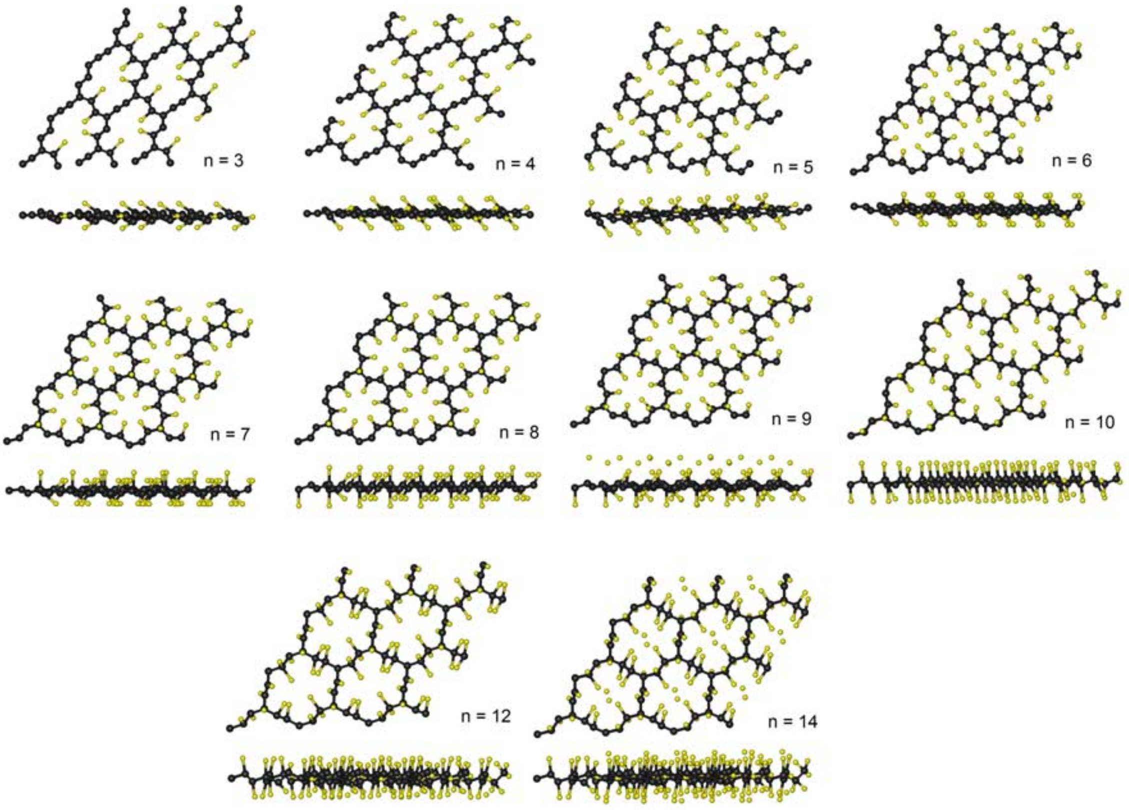

Fig. 5. Optimized atomic structures for the layers of the most stable isomers of chlorgraphynes C_8Cl_n with different Cl content (top and side views are depicted)

level is hosted at the band of Cl states, i.e. the system contains the free Cl radicals (Fig. 4, n = 14).

In addition, the low kinetic stability of the highly numbered C_8Cl_n chlorgraphynes may be traced using the relative difference in the formation energies between parent and daughter structures $\Delta E_n - \Delta E_{n-1}$ (Fig. 3). As it might be expected, the formation of compounds with open-shell electronic structure (the case of odd-numbered chlorgraphynes) is hindered and the difference in ΔE_n is always positive. Though, even-numbered chlorgraphynes with closed-shell electronic structure have negative values only up to the stoichiometry $C/Cl = 8/6$, the formation of chlorgraphynes with a higher Cl may be prohibited despite negative values for the calculated formation energies.

4. Summary

In summary, we have investigated the trends in stability, structural, and electronic properties of the proposed chlorinated graphynes (chlorgraphynes) with variable C/Cl stoichiometry up to composition C_8Cl_{14}, which is much higher than C/F ratio for "classical" fluorographene ($C/F = 1$) and could give an opportunity for the larger modulation of the properties and the engineering of a rich family of novel 2D materials.

Our DFT calculations have revealed the phenomena, which could occur during saturation of graphyne sheets by Cl atoms. We have considered a limited number of stoichiometries, isomers and conformers among the family of chlorinated α-graphynes and established a possible path for the formation of these compounds. The joint analysis of the structure, stability and electronic properties for a given stoichiometry uncovers the competition between electronic and steric factors. In contrast to the fluorine and hydrogen derivatives of graphene or graphynes [14,34], the maximal chemical saturation of graphyne layers by chlorine atoms should be prohibited due to the larger atomic radius of Cl. The maximal degree of chlorination would be likely possible only up to the composition C_8Cl_8 instead of nominal C_8Cl_{14}.

The most stable chlorgraphynes were found to be semiconductors, irrespective of their stoichiometry. The near Fermi level bands in C_8Cl_n monolayers are composed mainly of the $2p_z$C states, which can be assembled into a π-conjugated system in different manner. The found significance of steric factor in the formation of chlorgraphynes suggests also that the variety of the possible ad-atom arrangements would be much impoverished, than for their F- and H-substituted counterparts, and a more precise regulation of the structure may be achieved. Thus, the chlorination could be a more attractive route for the fabrication of graphyne layers with specific arrangement of ad-atoms and, consequently, tuned electronic and transport properties, than fluorination or hydrogenation.

Acknowledgments

The support of the RFBR project 13-03-00272- is gratefully acknowledged.

References

[1] Geim A.K., Novoselov K.S. The rise of graphene. *Nature Materials*, **6**, P. 183–191 (2007).

[2] Castro Neto A.H., Guinea N.M., Peres N.M.R., Novoselov K.S., Geim A.K. The electronic properties of graphene. *Reviews of Modern Physics*, **81**, P. 109–162 (2009).

[3] Castro Neto A.H. The carbon new age. *Materials Today*, **13**, P. 12–17 (2010).

[4] Soldano C., Mahmood A., Dujardin E. Production, properties and potential of graphene. *Carbon*, **48**, P. 2127–2150 (2010).

[5] Rozkov A.V., Giavaras G., Bliokh Y.P., Freilikher V., Nori F. Electronic properties of mesoscopic graphene structures: Charge confinement and control of spin and charge transport. *Physics Reports*, **503**, P. 77–114 (2011).

[6] Castro Neto A.H., Novoselov K.S. New directions in science and technology: two-dimensional crystals. *Reports on Progress in Physics*, **74**, P. 082501 (2011).

[7] Huang X., Yin Z., Wu S., Qi X., He Q., Zhang Q., Yan Q., Boey F., Zhang H. Graphene-based materials: synthesis, characterization, properties, and applications. *Small*, **7**, P. 1876–1902 (2011).

[8] Singh V., Joung D., Zhai L., Das S., Khondaker S.I., Seal S. Graphene based materials: past, present and future. *Progress in Materials Science*, **56**, P. 1178–1271 (2011).

[9] Nair R.R., Ren W.C., Jalil R., Riaz I., Kravets V.G., Britnell L., Blake P., Schedin F., Mayorov A.S., Yuan S., Cheng H.M., Strupinski W., Bulusheva L.G., Okotrub A.V., Grigorieva I.V., Grigorenko A.N., Novoselov K.S., Geim A.K. Fluorographene: a two-dimensional counterpart of teflon. *Small*, **6**, P. 2877–2884 (2010).

[10] Robinson J.T., Burgess J.S., Junkermeier C.E., Badescu S.C., Reinecke T.L., Perkins F.K., Zalalutdinov M.K., Baldwin J.W., Culbertson J.C., Sheehan P.E., Snow E.S. Properties of fluorinated graphene films. *Nano Letters*, **10**, P. 3001–3005 (2010).

[11] Zboril R., Karlicky F., Bourlinos A.B., Steriotis T.A., Stubos A.K., Georgakilas V., Safarova K., Jancik D., Trapalis C., Otyepka M. Graphene fluoride: a stable stoichiometric graphene derivative and its chemical conversion to graphene. *Small*, **6**, P. 2885–2891 (2010).

[12] Jeon K., Lee Z., Pollak E., Moreschini L., Bostwick A., Park C.M., Mendelsberg R., Radmilovic V., Kostecki R., Richardson T.J., Rotenberg E. Fluorographene: a wide bandgap semiconductor with ultraviolet luminescence. *ACS Nano*, **5**, P. 1042–1046 (2011).

[13] Withers F., Russo S., Dubois M., Craciun M.F. Tuning the electronic transport properties of graphene through functionalisation with fluorine. *Nanoscale Research Letters*, **6**, P. 526 (2011).

[14] Leenaerts O., Peelaers H., Hernandez-Nieves A.D., Partoens B., Peeters F.M. First-principles investigation of graphene fluoride and graphane. *Physical Review B*, **82**, P. 195436 (2010).

[15] Withers F., Dubois M., Savchenko A.K. Electron properties of fluorinated single-layer graphene transistors. *Physical review B*, **82**, P. 073403 (2010).

[16] Samarakoon D.K., Chen Z., Nicolas C., Wang X.Q. Structural and Electronic Properties of Fluorographene. *Small*, **7**, P. 965–969 (2011).

[17] Artyukhov V.I., Chernozatonskii L.A. Structure and Layer Interaction in Carbon Monofluoride and Graphane: A Comparative Computational Study. *The Journal of Physical Chemistry A*, **114**, P. 5389–5396 (2010).

[18] Enyashin A.N., Ivanovskii A.L. Graphene allotropes. *Physica Status Solidi (b)*, **248**, P. 1879–1883 (2011).

[19] Baughman R.H., Eckhardt H., Kertesz V. Structure-property predictions for new planar forms of carbon: layer phases containing sp^2 and sp atoms. *Journal of Chemical Physics*, **87**, P. 6687–6699 (1987).

[20] Narita N., Nagai S., Suzuki S., Nakao K. Electronic structure of three-dimensional graphyne. *Physical Review B*, **62**, P. 11146–11151 (2000).

[21] Coluci V.R., Braga S.F., Legoas S.B., Galvao D.S., Baughman R.H. Families of carbon nanotubes: graphyne-based nanotubes. *Physical Review B*, **68**, P. 035430 (2003).

[22] Kang J., Li J., Wu F., Li S.S., Xia J.B. Elastic, Electronic, and optical properties of two-dimensional graphyne sheet. *The Journal of Physical Chemistry C*, **115**, P. 20466–20470 (2011).

[23] Srinivasu K., Ghosh S.K. Graphyne and graphdiyne: promising materials for nanoelectronics and energy storage applications. *The Journal of Physical Chemistry C*, **116**, P. 5951–5956 (2012).

[24] Zhang H., Zhao M., He X., Wang Z., Zhang X., Liu X. High mobility and high storage capacity of lithium in sp–sp^2 hybridized carbon network: the case of graphyne. *The Journal of Physical Chemistry C*, **115**, P. 8845–8850 (2011).

[25] Pan L.D., Zhang L.Z., Song B.Q., Du S.X., Gao H.J. Graphyne- and graphdiyne-based nanoribbons: Density functional theory calculations of electronic structures. *Applied Physics Letters*, **98**, P. 173102 (2011).

[26] Malko D., Neiss C., Vines F., Gorling A. Competition for graphene: graphynes with direction-dependent dirac cones. *Physical Review Letters*, **108**, P. 086804 (2012).

[27] Hohenberg P., Kohn W. Inhomogeneous electron gas. *Physical Review B*, **136**, P. 864–871 (1964).

[28] Ordejon P., Artacho E., Soler J.M. Self-consistent order-N density-functional calculations for very large systems. *Physical Review B*, **53**, P. R10441 (1996).

[29] Soler J., Artacho E., Gale J.D., Garcia A., Junquera J., Ordejon P., Sanchez-Portal D. The SIESTA method for ab initio order-N materials simulation. *Journal of Physics: Condensed Matter*, **14**, P. 2745–2779 (2002).

[30] Perdew J.P., Zunger A. Self-interaction correction to density-functional approximations for many-electron systems. *Physical Review B*, **23**, P. 5048–5079 (1981).

[31] Troullier N., Martins J.L. Efficient pseudopotentials for plane-wave calculations. *Physical Review B*, **43**, P. 1993–2006 (1991).

[32] Moreno J., Soler J.M. Optimal meshes for integrals in real- and reciprocal-space unit cells. *Physical Review B*, **45**, P. 13891–13898 (1982).

[33] Monkhorst H., Pack J.D. Special points for Brillouin-zone integrations. *Physical Review B*, **13**, P. 5188–5192 (1976).

[34] Enyashin A.N., Ivanovskii A.L. Fluorinated derivatives of sp^2 carbon allotropes: Structure, stability and electronic properties. *Chemical Physics Letters*, **545**, P. 78–82 (2012).